Infinitesimally Shape-Similar Motions Using Relative Angle Measurements

Ian Buckley and Magnus Egerstedt

***Abstract*— This paper revisits the formation control problem, whereby a team of mobile robots assemble and maintain a desired geometric shape. However, the types of shapes that are realizable by a given robot team depends directly on the sensing modalities of the individual robots. For example, rigidity-based approaches make use of distance measurements, and the idea is to restrict the motion of the robots so that all inter-robot distances are maintained, thereby ensuring purely rigid motion. Rather than distances, we notice that for certain sensor classes, such as monocular pinhole cameras, only relative angle measurements are available. To this end, we introduce the notion of shape-similar motions, which constitutes a class of angle preserving motions that also preserve the shape of the formation in the sense that rigid motions as well as uniform scalings are permissible. We construct the shape-similarity matrix, whose null-space captures angle preserving motions, and show that by restricting the dimension of the null-space, we can guarantee that motions of the formation preserve the shape. Lastly, we implement a shape-similar controller on a team of differential drive mobile robots.**

***Index Terms*— Multi-Robot Systems**

I. Introduction

Formation control is typically concerned with the problem of designing appropriate coordinated control strategies for assembling and maintaining desired geometric shapes. A number of successful formation control strategies have been developed for a wide range of platforms and performance objectives, e.g., [1] [2] [3]. However, the shapes that can be produced by a team of robots are ultimately determined by sensing capabilities (What type of information do individual robots have about adjacent agents?), mobility considerations (What type of motions can the robots execute?), and environmental factors (How are environmental constraints and conditions influencing the capabilities of the robots?). In this paper, we consider the first of these issues and focus on a particular coupling between sensing capabilities and the corresponding shapes that the team can maintain.

For mobile ground robots, a rich body of work has been developed on formation control based on range and bearing sensors, i.e., if two robots are located at positions $x_i, x_j \in \mathbb{R}^2$ [1], then the information available to robot i is the displacement of robot j relative to robot i, i.e., $x_j - x_i$. For example, if the desired distance between robots i and j is given by d_{ij}, a standard controller would be of the form

$$\dot{x}_i = \sum_{j \in N_i} F(\|x_i - x_j\| - d_{ij})(x_j - x_i),$$

where $\dot{x}_i$ is the velocity of robot i, N_i is the set of neighboring robots measurable by robot i, and $F : \mathbb{R} \to \mathbb{R}$ is a monotonically increasing function with $F(0) = 0$ as discussed in [4]. In fact, one reason range and bearing information has been used in a number of multi-robot applications is that this information can (roughly) be obtained through standard range-sensor skirt configurations, i.e., where range sensors (e.g. IR, LIDAR, ultrasonic) are distributed around the body of the robot, or by stereo vision sensing modalities. Another reason why this information is particularly useful is that it does not require knowledge of the actual positions of the robots, i.e., robot i does not need to know x_i [5].

A variant of this is when only range information is available, i.e., when only the distance $\|x_i - x_j\|$ is available to the robots. This is, for example, the case when received transmission power between communicating robots is used as a proxy for distance as was discussed in [6]. When only distance information is available, so-called *rigidity*-based control strategies have been developed for ensuring that the team maintains the proper inter-robot distances while maneuvering [7] [8].

Formation control strategies based on rigidity draw from the wealth of work on graph rigidity [9] [10] [11] [12]. If we let the index-set to a team of n robots be given by $V = \{1, \ldots, n\}$ and assume that $E \subset V \times V$ is a set of unordered pairs of edges to be maintained, a distance-preserving motion is one that satisfies

$$\frac{d}{dt}\frac{1}{2}\|x_i - x_j\|^2 = (x_i - x_j)^T(\dot{x}_i - \dot{x}_j) = 0, \; \forall (i,j) \in E. \quad (1)$$

Stacking the robot states together as $x = [x_1^T, \ldots, x_n^T]^T$ we can write the above condition in a more compact and convenient form, $R(x)\dot{x} = 0$. If the robots are planar, the number of edges to preserve is k, and there are n robots in the team, $R(x)$ is a $k \times 2n$-matrix known as the rigidity-matrix [10]. The elegance of this formulation is that it exactly captures when a motion preserves the distances between the specified pairs of robots; that is, a motion is distance-preserving if and only if it lies in the null-space of the rigidity matrix, i.e. $\dot{x} \in \ker(R(x))$. However, this fact alone does not guarantee that the shape of the formation is preserved because while a set of pairwise distances is maintained, it

Email: {ihbuckl,magnus}@gatech.edu

School of Electrical and Computer Engineering, Georgia Institute of Technology, Atlanta, GA 30332, USA.

[1] In this paper we consider planar robots, but a significant part of the developments generalize to higher dimensions as well.

does not follow that the shape is maintained [2] For example, in a line formation, each pair can be maintained while the line collapses on itself.

Intuitively, sufficiently many inter-robot distances need to be maintained or the shape of the formation could be distorted, i.e., the formation could be flexible [13]. One solution is to maintain all possible inter-robot distances, but for practical reasons, we are more interested in maintaining a subset of distances $d/dt\|x_i - x_j\| = 0,\ (i,j) \in E$, such that *all* pairwise distances are maintained, i.e., $d/dt\|x_i - x_j\| = 0,\ \forall (i,j) \in V \times V$.

In the plane, rigid motions consist of 2D-translations and a 1D-rotation. In other words, motions of rigid bodies have exactly three degrees of freedom. This means that if $\dim(\ker(R(x))) > 3$, it is possible to maintain inter-robot distances while moving in such a way that the formation does not behave as a rigid body. One of the more elegant results from rigidity theory states that (V,E) is generically, infinitesimally rigid if and only if $\dim(\ker(R(x))) = 3$ [9], where the modifiers "generically" and "infinitesimally" refer to the fact that x should stay away from degenerate configurations (such as co-linear) and the motions have to be continuous, respectively. This restriction on the dimension of the null-space of the rigidity matrix constrains the motions of the robots to those that both preserve the inter-agent distances and the rigidity of the formation.

In this paper, we consider robots that, for whatever reason (e.g. design, cost, etc.), can only measure angles–how can formations be achieved with such robots? To avoid defining and maintaining a global reference, which either requires precise compass measurements or known landmarks, we assume that robot k can "see" robots i and j, i.e. the angle θ_{ikj} between $x_i - x_k$ and $x_j - x_k$ centered on x_k can be measured as shown in Figure 1. Under this construction, one option for obtaining this bearing information is monocular vision. Figure 2 depicts a simplified model of a pinhole camera mounted on robot k. Assuming knowledge of the intrinsic camera parameters, the angle θ_{ikj} can be determined using the pixel coordinates $\tilde{x}_i$ and $\tilde{x}_j$ of robots i and j.

Sensors that yield angle measurements, such as cameras, impose interesting complications on the task of achieving formation. By only measuring the relative angles between robots, uniform scaling of the formation will maintain the angles, but will alter the inter-agent distances. Thus, it is not possible to guarantee rigidity using angle measurements alone. Related to angle measurements, but explicitly referencing the coordinate frame, are bearings (unit vectors formed by the difference of agent states, i.e., $(x_j - x_i)/\|x_j - x_i\|\ \forall (i,j) \in E$), which are used in bearing-rigidity theory to determine whether frameworks are the same under uniform scalings and translations of the framework, but not rotations [14]. In this paper, we introduce shape-similarity, a departure from both rigidity and bearing-rigidity that allows us to scale the formation and apply rigid motions while guaranteeing that the relative inter-agent distances and angles have been maintained.

[2]Throughout the paper, "shape" refers to the particular scaling and angles of the framework rather than to classes of objects that share common angles.

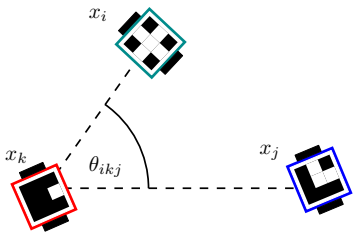

Fig. 1: The angle θ_{ikj} between robots x_i and x_j is centered on x_k.

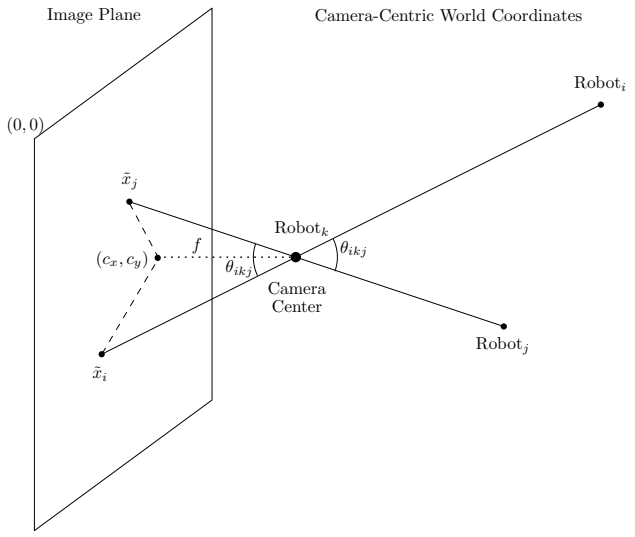

Fig. 2: A simplified pinhole camera model shows how a camera mounted on robot k could be used to measure the angle between robots i and j. The robots i and k are projected from 3D through the camera center at robot k onto the 2D image plane. Using knowledge of the camera parameters, such as the focal length f and the camera center projected onto the image plane (c_x, c_y), it is possible to determine θ_{ikj} using the pixel coordinates $\tilde{x}_i$ and $\tilde{x}_j$.

II. Angle Preserving Motions

In this section, we characterize the set of motions that preserve the relative angles in a manner akin to the discussion of rigidity, and as with rigidity, ensuring that motions of the robots preserve inter-agent distances is not sufficient to guarantee that the shape of the formation is maintained–the space of distance preserving motions is restricted to rigid motions of the formation. In this section, we draw inspiration from this development and define a class of motions that preserve the angles in a formation while preserving the shape. We begin by formally introducing key terminology, which we use throughout the paper. Finally, we introduce shape-similarity.

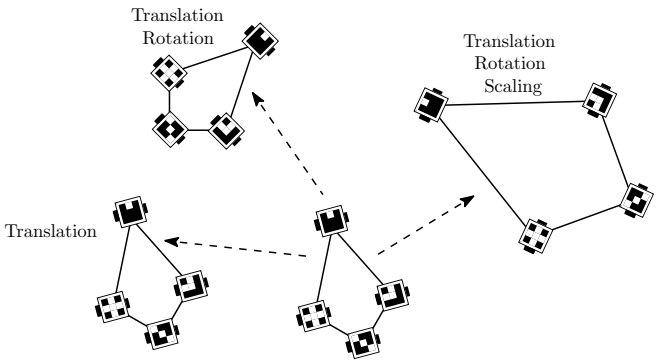

Fig. 3: By maintaining angles along trajectories, translating, rotating, and scaling will preserve the shape of the framework.

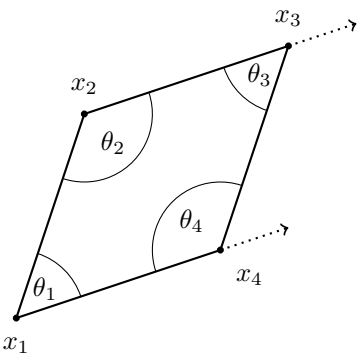

Fig. 4: Angle-consistent trajectories (dotted lines) of the formation above do not preserve the shape.

A. Formation Specification

As in the introduction, let $V = \{1, \ldots, n\}$ be a set of robot indices associated with a team of planar robots, and let $E \subset V \times V$ be a set of unordered pairs, with the interpretation that $(i, k) \in E$ and $(k, j) \in E$ means that the angle θ_{ikj} is to be preserved. Moreover, assume that the robots are located at $x_i,\ i = 1, \ldots, n$. Following the notion in [4], we refer to the set of locations together with the graph $G = (V, E)$ as a framework $G(x)$ (an alternative term for this is an embedded graph, as discussed in [15]).

We are interested in characterizing the conditions for which all (infinitesimal) motions that preserve the relative angles ensure that only scalings and rigid transformations of the shape can result. To this end, we need the notion of shape-similarity.

B. Shape-Similarity

Because we are considering bearing-based sensing, we are interested in maintaining the shape by ensuring that the angles of the framework do not change. A trajectory of the framework $G(x)$ is said to be *angle-consistent* if angles are maintained. Having introduced angle-consistency, we now define shape-similarity.

Definition 1. *A framework $G(x)$ is infinitesimally shape-similar if all angle-consistent trajectories only result in rigid transformations and uniform scalings of the shape.*

By the definition of shape-similarity and its relationship to geometric similarity, in the plane, there are exactly 4 degrees of freedom, as illustrated in Figure 3. In subsequent sections, this observation will play a major role when analyzing and characterizing shape similar motions.

III. The Shape-Similarity Matrix

To show that a framework is rigid, it is sufficient to show that the edge distances do not change along trajectories. Unfortunately, it is not possible to take such a straight-forward approach to demonstrate shape-similarity along trajectories. Instead, we capture shape-similarity by first considering angle-consistent motions, which are a superset of shape-similar motions.

From the definition of angle-consistency, we know that shape-similar motions are angle-consistent. The reverse does not necessarily hold; depending on the framework, it may be possible to maintain angles while distorting the shape. To illustrate this point, consider the planar framework shown in Figure 4; this framework is not shape-similar because the agents x_3 and x_4 can move along the dotted lines, which is an angle-consistent motion that does not preserve the shape. In order to establish conditions under which a framework is necessarily angle-consistent and shape-similar, we must first determine the conditions for which infinitesimal motions of the framework are angle-consistent.

We begin by considering m angles of the framework along trajectories specified by the edges in the formation graph G. Without loss of generality, we choose a particular angle $\theta_{ikj}(t)$. The three agents defining $\theta_{ikj}(t)$ are $x_i(t)$, $x_j(t)$, and $x_k(t)$. Recognizing that the angle $\theta_{ikj}(t)$ can be written in terms of the inner product of the vectors $(x_i(t) - x_k(t))$ and $(x_j(t) - x_k(t))$, which lie along the edges of the framework, the expression for $\theta_{ikj}(t)$ becomes

$$\theta_{ikj}(t) = \cos^{-1}\left(\frac{\langle x_i(t) - x_k(t), x_j(t) - x_k(t)\rangle}{\|x_i(t) - x_k(t)\|\|x_j(t) - x_k(t)\|}\right), \quad (2)$$

where we use f to denote the expression inside the parenthesis above.

The angle θ_{ikj} is preserved along trajectories of the framework[3] if $\dot{\theta}_{ikj} = 0$. Taking the derivative, we have

$$\dot{\theta}_{ikj} = -\dot{f}(x_i, x_j, x_k)/\sqrt{1 - (f(x_i, x_k, x_j))^2} \quad (3)$$

$$= \alpha \dot{f}(x_i, x_j, x_k). \quad (4)$$

Taking the derivative of f with respect to time gives,

$$\dot{f}(x_i, x_j, x_k) = \frac{\partial f(x_i, x_j, x_k)}{\partial x_i}\dot{x}_i + \frac{\partial f(x_i, x_j, x_k)}{\partial x_j}\dot{x}_j + \frac{\partial f(x_i, x_j, x_k)}{\partial x_k}\dot{x}_k, \quad (5)$$

[3]Time dependence of the agents is omitted for notational convenience.

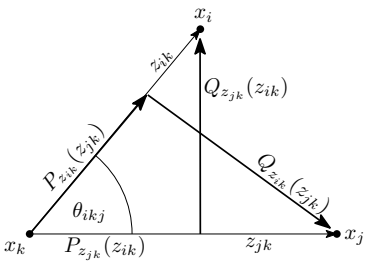

Fig. 5: The agents (x_i, x_k, and x_j), the vectors (z_{ik} and z_{jk}), the projections of these vectors onto each other ($P_{z_{ik}}(z_{jk})$ and $P_{z_{jk}}(z_{ik})$), and their orthogonal components to each other ($Q_{z_{ik}}(z_{jk})$ and $Q_{z_{jk}}(z_{ik})$) are shown.

and solving for the partial derivatives, we find:

$$\begin{aligned}\dot{f}(x_i,x_j,x_k) = \\ &\left(\frac{(x_j-x_k)^T - \frac{\langle x_i-x_k, x_j-x_k\rangle}{\|x_i-x_k\|^2}(x_i-x_k)^T}{\|x_i-x_k\|\|x_j-x_k\|}\right)\dot{x}_i \\ &+\left(\frac{(x_i-x_k)^T - \frac{\langle x_i-x_k, x_j-x_k\rangle}{\|x_j-x_k\|^2}(x_j-x_k)^T}{\|x_i-x_k\|\|x_j-x_k\|}\right)\dot{x}_j \\ &+\left(\frac{(2x_k-x_i-x_j)^T}{\|x_i-x_k\|\|x_j-x_k\|}\right)\dot{x}_k \\ &+\left(\frac{\langle x_i-x_k, x_j-x_k\rangle\left(\frac{(x_i-x_k)^T}{\|x_i-x_k\|^2}+\frac{(x_j-x_k)^T}{\|x_j-x_k\|^2}\right)}{\|x_i-x_k\|\|x_j-x_k\|}\right)\dot{x}_k.\end{aligned} \tag{6}$$

Rewriting (6) using $z_{ik} = (x_i - x_k)$ and $z_{jk} = (x_j - x_k)$; defining the projection of z_{jk} onto z_{ik} as

$$P^T_{z_{ik}}(z_{jk}) := \frac{\langle z_{ik}, z_{jk}\rangle}{\|z_{ik}\|^2} z^T_{ik};$$

and defining the orthogonal component of the vector z_{jk} to z_{ik} to be

$$Q_{z_{ik}}(z_{jk}) := z_{jk} - P_{z_{ik}}(z_{jk}),$$

(6) can be written in matrix form as:

$$\begin{aligned}\dot{f}(x_i,x_j,x_k) = \\ &\begin{bmatrix}\frac{Q^T_{z_{ik}}(z_{jk})}{\|z_{ik}\|\|z_{jk}\|} & \frac{Q^T_{z_{jk}}(z_{ik})}{\|z_{ik}\|\|z_{jk}\|} & \frac{-Q^T_{z_{ik}}(z_{jk})-Q^T_{z_{jk}}(z_{ik})}{\|z_{ik}\|\|z_{jk}\|}\end{bmatrix}\begin{bmatrix}\dot{x}_i\\ \dot{x}_j\\ \dot{x}_k\end{bmatrix},\end{aligned} \tag{7}$$

where the corresponding projections are depicted in Figure 5. For convenience, we define:

$$K(z_{ik}, z_{jk}) := -Q^T_{z_{ik}}(z_{jk}) - Q^T_{z_{jk}}(z_{ik}). \tag{8}$$

Substituting (7) into (4),

$$\dot{\theta}_{ikj} = \alpha\begin{bmatrix}\frac{Q^T_{z_{ik}}(z_{jk})}{\|z_{ik}\|\|z_{jk}\|} & \frac{Q^T_{z_{jk}}(z_{ik})}{\|z_{ik}\|\|z_{jk}\|} & \frac{K(z_{ik},z_{jk})}{\|z_{ik}\|\|z_{jk}\|}\end{bmatrix}\begin{bmatrix}\dot{x}_i\\ \dot{x}_j\\ \dot{x}_k\end{bmatrix}, \tag{9}$$

and pulling out the scalar values $\lambda_{ikj} = \alpha/(\|z_{ik}\|\|z_{jk}\|)$, we are left with:

$$\dot{\theta}_{ikj} = \lambda_{ikj}\begin{bmatrix}Q^T_{z_{ik}}(z_{jk}) & Q^T_{z_{jk}}(z_{ik}) & K(z_{ik},z_{jk})\end{bmatrix}\begin{bmatrix}\dot{x}_i\\ \dot{x}_j\\ \dot{x}_k\end{bmatrix}. \tag{10}$$

Repeating this process for m angles specifying the formation of n agents, (10) takes the form:

$$\dot{\theta} = \Lambda M(x)\dot{x} = 0, \tag{11}$$

where $\Lambda \in \mathbb{R}^{m\times m}$ is a diagonal matrix containing the scaling associated with each angle in the formation λ_{ikj}, and $\dot{x} \in \mathbb{R}^{2n}$ is the vector of the infinitesimal motions of the framework. $M(x) \in \mathbb{R}^{m\times 2n}$ is the *shape-similarity matrix*. The structure of $M(x)$ follows from the derivation. An element in $M(x)$, $m_{pq} \in \mathbb{R}^{1\times d}$, corresponds to the component of the p^{th} angle contributed by agent q–if agent q does not contribute to angle p, $m_{pq} = 0$. For example, the shape-similarity matrix for the framework in Figure 4 is

$$\begin{aligned}M(x) = \\ &\begin{bmatrix}K(z_{41},z_{21}) & Q^T_{z_{21}}(z_{41}) & 0 & Q^T_{z_{41}}(z_{21})\\ Q^T_{z_{12}}(z_{32}) & K(z_{12},z_{32}) & Q^T_{z_{32}}(z_{12}) & 0\\ 0 & Q^T_{z_{23}}(z_{43}) & K(z_{23},z_{43}) & Q^T_{z_{43}}(z_{23})\\ Q^T_{z_{14}}(z_{34}) & 0 & Q^T_{z_{34}}(z_{14}) & K(z_{14},z_{34})\end{bmatrix}.\end{aligned}$$

By construction of the shape-similarity matrix, we have proved the following statement:

Theorem 1. *The null-space of the shape-similarity matrix $M(x)$ is the space of angle-consistent infinitesimal motions $\dot{x}$ of the framework $G(x)$.*

The construction of the shape-similarity matrix was predicated on the fact that shape-similar motions are a subset of angle-consistent motions and that depending on the structure of the framework, there may exist angle-consistent trajectories that do not maintain the shape. In fact, from Theorem 1, we know that $\ker(M(x))$ is the space of angle-preserving motions of the framework. We are interested in showing that by properly specifying the edges of the formation graph, which are used in turn to specify the angles of the framework, we can restrict the space of angle-preserving motions to that of shape-preserving motions. In particular, for a framework in $\mathbb{R}^2$ where we know that shape similar motions always have exactly 4 degrees of freedom, we have the following:

Corollary 1.1. *The framework $G(x)$ is infinitesimally shape-similar in the plane*[4] *if and only if* $\dim(\ker(M(x))) = 4$.

Corollary 1.1 is of practical interest when deciding which angles of the framework should be maintained. By choosing feasible values for the agents in the formation shown in Figure 4, we find that $\dim(\ker(M(x))) = 5$, which indicates that the framework is not shape-similar. Alternately, choosing

[4]As was done for rigidity, we can directly extend Corollary 1.1 frameworks in $\mathbb{R}^3$, where we have a similar result: the framework $G(x)$ is shape-similar in 3D if and only if $\dim(\ker(M(x))) = 7$.

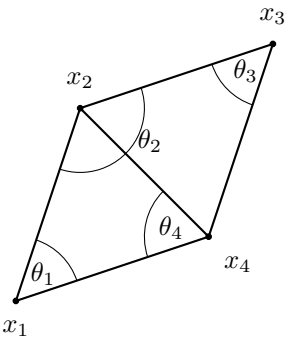

Fig. 6: A simple modification to the formation shown in Figure 4 results in shape-similarity

a different angle to maintain, as in Figure 6, results in a framework for which angle-consistent trajectories are exactly shape-similar, and as expected $\dim(\ker(M(x))) = 4$.

IV. Experiments

In this section, we demonstrate that the shape-similarity matrix is a practical tool that can be used to enforce shape-similar motions of agents in planar formations. We begin by considering simulations of planar agents with single-integrator dynamics of the form $\dot{x}(t) = u(t)$; we then demonstrate shape-similar formation control of a team of differential drive mobile robots.

A. Task

The particular scenario under consideration is to specify a target configuration of the formation which should be achieved while maintaining shape-similarity. For a feasible target configuration of the the agents x_d (i.e. a scaled, rotated, and translated realization of the initial framework), we consider the task of generating appropriate control inputs for the agents. In particular, we are interested in the minimization:

$$\begin{aligned} \min_{u \in \mathbb{R}^{2n}} \quad & \frac{1}{2}\|u - u_d\|^2 \\ \text{s.t.} \quad & M(x)u = 0, \end{aligned} \tag{12}$$

where u is the control input, $u_d = x_d - x$ is the nominal proportional control input formed by the difference of the target configuration and the current state, and the equality constraint enforces shape-similarity. To complete the minimization, we form the Lagrangian

$$L(u, \lambda) = \frac{1}{2}\|u - u_d\|^2 + \lambda^T M(x)u, \tag{13}$$

where $\lambda \in \mathbb{R}^m$ is the Lagrange multiplier. Because the problem is convex, the necessary and sufficient condition for optimality is

$$\left(\frac{\partial L(u,\lambda)}{\partial u}\right)^T = u - u_d + M^T(x)\lambda = 0, \tag{14}$$

$$M(x)u = 0. \tag{15}$$

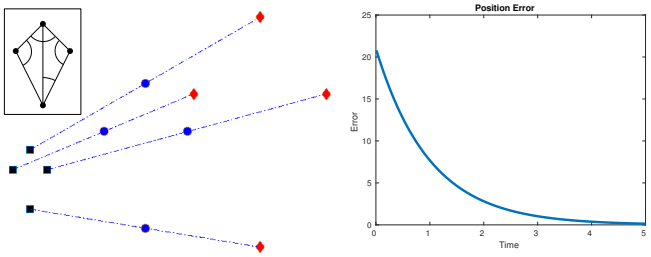

(a) (b)

Fig. 7: Figure 7a shows a shape-similar formation ($\dim(\ker(M(x))) = 4$) of single-integrator agents (blue circles) moving along trajectories (dashed blue lines) from the initial formation (black squares) to the target formation (red diamonds). The inset shows the angles maintained. Figure 7b shows that the position error approaches zero.

Solving first for the Lagrange multiplier and then for the control input, we find the minimal control input

$$u = (I - M^T(x)(M(x)M^T(x))^{-1}M(x)))u_d, \tag{16}$$

where $I \in \mathbb{R}^{n \times n}$ is an identity matrix, and the inverse of $M(x)M^T(x)$ is well-defined for all but pathological zero measure sets of the states $x(t)$.

B. Simulation

Four simulations are shown in Figures 7a, 8a, 8b and 8c. The formations of the first three simulations satisfy $\dim(\ker(M(x))) = 4$ and demonstrate that trajectories of the single integrators executing the control law derived in (16) are shape-similar. The formation in Figure 8c has $\dim(\ker(M(x))) > 4$ and is not shape-similar. The insets show the angles of the formations that are maintained.

Figure 7a shows the translation and scaling of a kite-shaped formation of four agents. Figure 7b shows that the error between the target configuration and the state, $\|x(t) - x_d\|$, decays to 0 for the kite-shaped formation.

Figure 8a shows the translation, rotation, and scaling of a formation of six agents, and Figure 8b shows that shape-similarity is maintained despite the fact that an infeasible

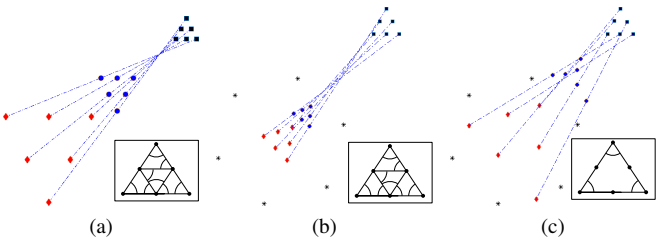

(a) (b) (c)

Fig. 8: Figure 8a shows a shape-similar formation satisfying $\dim(\ker(M(x))) = 4$. Figure 8b shows that the formation is shape-similar despite an infeasible target configuration (black stars). Figure 8c shows that the framework is not shape-similar if $\dim(\ker(M(x))) > 4$.

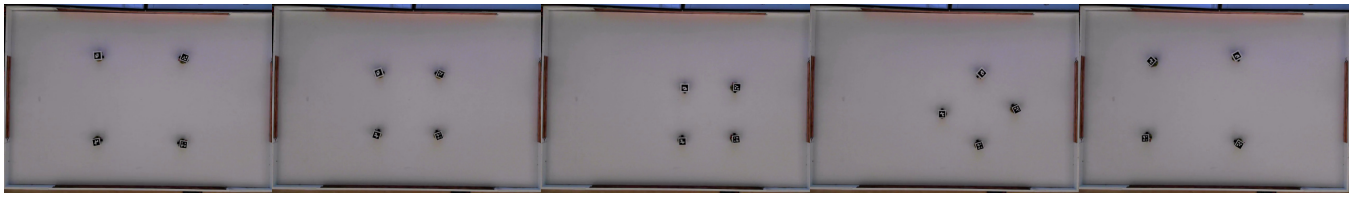

Fig. 9: The formation control law (16) was implemented on a team of four differential drive robots. From left-to-right, the robots initialize, scale by 60%, translate -0.2m, rotate 45°, and finally, rotate 45°, translate 0.2m, and scale by 170%.

target configuration was specified. In contrast, Figure 8c shows that if the formation, or equivalently, the shape-similarity matrix, is poorly constructed, motions of the agents may not preserve the desired shape of the formation. In this simulation, the shape is clearly distorted along the trajectory.

As demonstrated by the simulations, the developments of Section III are useful in achieving formations of single-integrators capable of translation, rotation, and scaling while maintaining the desired shape. Theorem 1 was used to develop a control law that preserves the shape of the formation, and Corollary 1.1 was used to inform the choice of angles in the frameworks that maintain shape-similarity.

C. Robot Experiments

The formation control law (16) was implemented on the Robotarium [16], a remotely accessible swarm robotics testbed. The purpose of the experiment was to demonstrate that the developments of Section III provide practical tools for enforcing shape-similar formations of robots.

Because of the non-holonomic constraints of the differential drive robots, it is not possible to directly apply in (16). Modelling these robots with unicycle dynamics

$$\dot{x} = v\cos(\theta) \qquad \dot{y} = v\sin(\theta) \qquad \dot{\theta} = \omega, \tag{17}$$

we instead apply a mapping between the linear and rotational velocity control inputs of the differential drive robots, v and ω, and a point with single-integrator dynamics in the plane ($u = [u_1, u_2]^T$) a short distance l ahead of each robot

$$\begin{bmatrix} v \\ \omega \end{bmatrix} = \begin{bmatrix} \cos(\theta) & \sin(\theta) \\ -\sin(\theta)/l & \cos(\theta)/l \end{bmatrix} \begin{bmatrix} u_1 \\ u_2 \end{bmatrix}, \tag{18}$$

as was introduced in [17]. Under this mapping, the control law (16) was executed on the differential drive robots. Figure 9 shows sequential stills captured during an experiment in which four robots maintained four angles satisfying $\dim(\ker(M(x))) = 4$. For aesthetics, the robots were initialized to the square formation shown in leftmost image of Figure 9 (any non-degenerate initialization would work). The controller was used to drive the robots to a series of four desired configurations, which were chosen to fully demonstrate shape-similarity of the formation. From left-to-right, the formation scales about the origin, translates, rotates, and finally, simultaneously translates, rotates, and scales.

V. Conclusions

In this paper, we demonstrated that by using relative angle measurements it is possible to maintain the shape of a formation along trajectories that translate, rotate, and scale the formation. We developed the shape-similarity matrix and showed that for planar formations, motions of the agents in the null-space of the shape-similarity matrix are exactly shape preserving if and only if the dimension of the null-space of the shape-similarity matrix is 4. The ability to scale the formation while guaranteeing that the shape is preserved is an exciting quality of the shape-similarity matrix that can be leveraged in formation control.

References

[1] J. R. T. Lawton, R. W. Beard, and B. J. Young, "A decentralized approach to formation maneuvers," *IEEE Trans. Robot. Autom.*, vol. 19, no. 6, pp. 933–941, Dec 2003.

[2] T. H. A. van den Broek, N. van de Wouw, and H. Nijmeijer, "Formation control of unicycle mobile robots: a virtual structure approach," in *IEEE Proc. Conf. Decision and Control*, Dec 2009, pp. 8328–8333.

[3] K. Oh, M. Park, and H. Ahn, "A survey of multi-agent formation control," in *Automatica*, vol. 53, March 2015, pp. 424–440.

[4] M. Mesbahi and M. Egerstedt, *Graph Theoretic Methods in Multiagent Networks*, 2010.

[5] F. Bullo, J. Cortéz, and S. Martínez, *Distributed Control of Robotic Networks: A Mathematical Approach to Motion Coordination Algorithms*, 2009.

[6] C. Filoramo, A. Gasparri, F. P. adn A. Priolo, and G. Ulivi, "A RSSI-based technique for inter-distance computation in multi-robot systems," in *18th Mediterranean Conf. Control Autom.*, June 2010, pp. 957–962.

[7] T. Eren, W. Whiteley, B. D. O. Anderson, A. S. Morse, and P. N. Belhumeur, "Information structures to secure control of rigid formations with leader-follower architecture." in *IEEE Proc. Amer. Control Conf.* IEEE, 2005, pp. 2966–2971.

[8] T. Eren, P. N. Belhumeur, B. D. O. Anderson, and A. S. Morse, "A framework for maintaining formations based on rigidity," *IFAC Proc. Volumes*, vol. 35, no. 1, pp. 499–504, 2002.

[9] H. Gluck, "Almost all simply connected closed surfaces are rigid," *Lecture Notes in Math*, vol. 438, pp. 225–239, 1975.

[10] L. Asimov and B. Roth, "The rigidity of graphs," in *Trans. Amer. Math. Soc.*, vol. 245, 1978, pp. 249–289.

[11] G. Laman, "On graphs and rigidity of plane skeletal structures," *J. Eng. Math.*, vol. 4, pp. 331–340, 1970.

[12] J. M. Hendrickx, B. D. O. Anderson, and V. D. Blondel, "Rigidity and persistence of directed graphs," in *IEEE Conf. on Decision and Control*, 2005, pp. 2176–2181.

[13] B. Roth, "Rigid and flexible frameworks," *The Amer. Math. Monthly*, vol. 88, no. 1, pp. 6–21, 1981.

[14] S. Zhao and D. Zelazo, "Bearing rigidity and almost global bearing-only formation stabilization," vol. 61, no. 5, pp. 1255–1268, 2016.

[15] J. M. McNew, E. Klavins, and M. Egerstedt, "Solving coverage problems with embedded graph grammars," in *Hybrid Systems: Computation and Control*. Springer, 2007, pp. 413–427.

[16] D. Pickem, P. Glotfelter, L. Wang, M. Mote, A. Ames, E. Feron, and M. Egerstedt., "The robotarium: A remotely accessible swarm robotics research testbed." in *IEEE Int. Conf. Robot. Autom.*, May 2017. to be published.

[17] R. Olfati-Saber, "Near-identity diffeomorphisms and exponential epsilon-tracking and epsilon-stabilization of first-order nonholonomic SE(2) vehicles," in *IEEE Proc. Amer. Control Conf.*, vol. 6, 2002, pp. 4690–4695.